ICARUS: Automatic Autonomous Power Infrastructure Inspection with UAVs

Antonis Savva, Angelos Zacharia, Rafael Makrigiorgis, Antreas Anastasiou, Christos Kyrkou, Panayiotis Kolios, Christos Panayiotou, and Theocharis Theocharides

***Abstract* — Power transmission and distribution networks mostly span across harsh environments and thus, frequent faults and failures are observed, increasing the maintenance costs, pressing the authorities to provide electricity continuously and uninterruptedly. To this end, thorough field inspections with skilled personnel are regularly conducted, which are labor-intensive, costly and slow, whereby efficiency and staff safety cannot be always ensured. UAVs stem as a promising solution for power infrastructure inspection; however, their use is mostly limited by the fact that a remote pilot is in control of flight and mission processes, rendering reliable data acquisition in short time interval a tedious task. Despite research efforts for automating inspection procedures, these have not been widely adopted. In this study, we address this challenge by developing a Power Distribution Network Inspection Platform Using UAVs (ICARUS), based on a vision-based artificial intelligence toolkit, that integrates multiple sensors and automates many tasks, such as detection, tracking and identification of infrastructure components, gathering reliable spatial/time data associated to these components autonomously, safely and fast.**

***Index Terms* — power line inspection, vision-based inspection, autonomous navigation, unmanned aerial vehicles, deep learning.**

I. Introduction

The heavy dependence of societies on electricity puts pressure on Electricity Authorities (EAs) for covering the increasing demands [1], [2]. To this end, power transmission and distribution networks are operated, including high voltage (HV), medium voltage (MV) and low voltage networks, which mostly span across harsh environments and are frequently exposed to extreme weather conditions [1], [3], [4]. In the majority of cases, power infrastructure is aged, inevitably leading to degradation, which in turn may cause fires and power outages [1], [4]. In the latter case, it has been estimated that half-hour and eight-hours blackouts in the US resulted in an average loss of about $16,000 and $94,000, respectively [4], while for some sectors, e.g. financial, the costs may reach the order of millions [5]. Finally, in an interconnected power grid, a local power outage is also likely to initiate a domino effect, affecting other regions as well [4].

To mitigate these effects, EAs proactively conduct thorough routine inspections with skilled personnel, which are dispatched across the power infrastructure either on foot or with helicopters [4]. Inspectors visually assess the condition of power components, by primarily employing binoculars and less frequently dedicated cameras to detect specific conditions, such as increased temperatures and corona effects [1], [4], [6]. While this inspection approach has been mainly applied worldwide, there are pros and cons of these methodologies, i.e. patrol vs. helicopter-based. The former allows for longer evaluation times; thus, increasing detection rates at the cost for shorter network coverage, while the latter allows the inspection of a larger portion of the network, due to the increased speed, at the cost of lower detection rates [1]. Both approaches are potentially dangerous for the staff, require skilled personnel, i.e. for inspecting the network and for flying helicopters, while efficiency depends on the observation skills of the inspectors and fatigue levels [4].

In this context, UAVs stem as a promising and flexible solution for power infrastructure inspection, due to their inherent capability of providing high-quality data of power components, by being able to carry high-end cameras and to fly close to power lines. Moreover, the associated operating costs are significantly lower compared to conventional helicopter-based approaches [1]. While the concept of using UAVs for power infrastructure inspection dates back almost 20 years ago [7], [8], significant attention has been given the last years, due to advances in UAV technology and their widespread commercial availability [1], [4]. Of particular interest is to build automatic and/or autonomous systems, with the ability to acquire data using multiple sensors, for better identifying defects in the network; however, such attempts had so far limited applicability [4]. These efforts are mainly constrained by the fact that a remote pilot is still in control of flight processes, e.g. data acquisition, by the ability to attach multiple payloads on the UAV, by computational limitations for real-time data processing, and by the large navigation and positioning error associated with a single Global Navigation Satellite System (GNSS), e.g. GPS [9]–[12].

In this study, we capitalize on recent advances in UAV technology and embedded hardware to develop ICARUS; a UAV-based platform which automates the inspection of power infrastructure network, both during data acquisition and analysis. With ICARUS, multiple sensors are integrated on the UAV, which is programmed to autonomously acquire data for mapping and identifying degradation conditions of the power distribution network. The developed system employs a hybrid navigation approach using multi-frequency and multi-constellation GNSSs to minimize navigation error, as well as deep learning algorithms for data analysis. Specifically, the employed UAV is equipped with an onboard embedded platform, which is responsible for real-time data processing to identify poles and record their accurate positions, since these are not precisely known. During inspection, ICARUS gathers data, which are subsequently processed with dedicated algorithms to identify insulators and their condition, to identify obstacles and assess vegetation

The authors are with the KIOS Research and Innovation Center of Excellence and the Department of Electrical and Computer Engineering, University of Cyprus, Nicosia, 1678, Cyprus. e-mails: {savva.d.antonis, zaxaria.angelos, makrigiorgis.rafael, anastasiou.antreas, kyrkou.christos, kolios.panayiotis, christosp, ttheocharides}@ucy.ac.cy.

near the power line corridor, to detect power lines, as well as to generate digital surface models.

II. Related Work

A. Vision-Based Inspection

In [8], the concept of a small autonomous robotic vehicle was introduced, which could detect the power lines for providing control and guidance feedback, also allowing to draw power from the lines [13]. Furthermore, unmanned autonomous helicopter (UAH) systems have been developed using both visible-light and infrared cameras for providing a more complete view of the condition of power components [14], [15]. In a similar research line, vision sensors were employed to develop UAH with obstacle detection and avoidance capabilities, using a stereo camera along with a laser scanner [16]. The progress in UAV technology allowed for incorporating additional sensors, such as Inertial Measurement Unit (IMU) and LIDAR scanner for detecting and following power lines [17]. Among vision-based approaches for power infrastructure inspection, two main categories can be distinguished based on: (i) power line and (ii) pole detection methodologies.

B. Inspection Based on Power Line Detection

The incentive for developing power line detection methods was for the UAV to be able to perform tracking and following tasks; thus, traversing the power infrastructure without the need of GNSS coordinates. To this end, a methodology was developed based on a pulse coupled neural filter for creating an edge map by removing noise in the background [18]. The resulted edge map was used as a prior to the Hough transform and a knowledge-based clustering method was applied in the Hough space to detect straight lines representing power lines [18]. In another study, power line detection was performed using steerable filters followed by a line fitting refinement step. Afterwards, a guidance approach was applied for generating suitable control commands to align the UAV's position directly above the power lines, with the lines being vertically oriented within the image [19]. In [20], a circle-based algorithm was developed for detecting power lines, which was subsequently expanded to additionally estimate their orientation and was employed in the design and development of an onboard navigation approach [21]. Conventional computer vision approaches, e.g. Hough transform, were employed in [22] to achieve real-time detection, while efforts in [23] were directed in proposing a methodology to automatically select optimal thresholds associated to those algorithms, based on certain power line characteristics. Apart from the aforementioned approaches, machine learning was also employed and a Convolutional Neural Network (CNN) was developed for detecting power lines in aerial images [24]. Recently, a fast single-shot line segment detector (LS-Net) was proposed, based on a feed-forward fully CNN to detect power lines, achieving a performance of 21.5 frames per second (FPS) on a state-of-the-art GPU [25]. A fast segmentation CNN was also employed, taking as input four channels, i.e. red, green, blue, infrared, leading to real-time detection (24 FPS) on a high-end GPU [26].

C. Inspection Based on Pole Detection

While there were many attempts on detecting power lines, pole detection approaches received so far less scientific attention [4]. The developed methods rely on identifying the position of the pole within each frame and subsequently fixate the camera to the detected objects, or estimate real world distances. In [27], a corner detection algorithm was employed for detecting corners of the top of the pole and a matching approach was proposed for tracking the detected features across a series of images, ultimately fixating camera on the detected pole. On similar grounds, in [28] a detection methodology was employed to extract features using Histograms of Oriented Gradients, which were subsequently fed into two multi-layer perceptrons [29]. The first was responsible for separating foreground from background, while the second was used to distinguish among four different types of poles. Finally, tracking over consecutive frames was achieved with a hierarchical tracking method, aiming to maintain the detected pole inside camera's Field of View (FOV) during inspection [28]. Pole detection was also performed in [30], where the Line Segment Detector (LSD) algorithm was employed for detecting line segments on a HV tower [31]. Following a matching procedure across a sequence of video frames, corresponding line segments were used to provide depth estimation based on the UAV's ego-motion.

D. Inspection Based on Integrated UAV Systems

The aforementioned vision-based methodologies focused on detecting either power lines or poles to facilitate UAV navigation and control. Power line detection methods still lack sufficient accuracy for employment in real inspection scenarios, while pole detection-based navigation received less attention by researchers, as pointed out in a recent literature review [4]. Consequently, few studies presented an integrated approach for addressing power infrastructure inspection needs, consisting of detection, mapping and monitoring of power components, e.g. poles, insulators, power lines, as well as vegetation monitoring [4]. To this direction, in [32] a UAV was developed to automatically inspect power components and identifying vegetation near the power line corridor, as well as poor conductivity and hotspots on these components. To accomplish inspection, three computers were employed, one for controlling the flight plan, telemetry and commands between the UAV and the ground station, one for receiving visible-light video feed to measure distance from power lines to the surrounding vegetation, and one for receiving video feed from the infrared camera for detecting temperature differences. Both video feeds were acquired at 4 FPS, while inspection was performed in two phases; during the UAV's flight to the designated position, as well as during its return to the take-off point. Specifically, the power lines were detected by applying basic computer vision algorithms, such as Otsu thresholding, morphological operations and Hough transform, with the resulting detections being subsequently used to estimate the distance between power lines and the UAV. The UAV's height was determined using a laser altimeter, while data from the vision sensors along with stereoscopic analysis were employed for estimating the distance between power lines and vegetation [32]. In a series of studies, a research team proposed and applied an autonomous navigation approach for HV power infrastructure inspection [9], by

Fig. 1: Equipment for implementing ICARUS inspection platform, consisting of the DJI Matrice 300 RTK UAV, the multi-sensor (RGB and thermal) DJI Zenmuse H20T camera (right downward gimbal), the MicaSense Altum multispectral camera (left downward gimbal) and the NVIDIA Jetson Xavier NX embedded platform (top of UAV; figure inset). Orange dotted and red dashed arrows indicate the differential RTK and transmission antennas, respectively.

detecting towers using the Faster Region-based CNN (Faster-RCNN) and the Kernelized Correlation Filters (KCF) for tracking across a sequence of images [10], [11]. In this context, Faster-RCNN was used to initially detect the tower and to correct tracking results obtained by KCF, due to the low processing speed (2 FPS) on the onboard hardware embedded module. Additionally, 2D images acquired from a monocular camera along with a projective model, were used to estimate velocity in 3D space, since GPS was not employed for navigation [12].

In this context, we capitalize on both pole detection methodologies with deep learning on an embedded platform to increase real-time processing speed, and multiple GNSSs to decrease navigation and positioning error. Consequently, the UAV autonomously navigates across the network (the pilot intervenes only in case of an emergency) without being supplied with the accurate locations of poles. During its mission, the UAV identifies each pole and records its accurate spatial position. Simultaneously, the integration of multiple sensors, facilitates the autonomous acquisition of various data, which are processed to identify degraded power components, to monitor vegetation and to map the power network. Within this framework, the development of all algorithms is performed without using dedicated hardware, e.g. high-end GPUs, to promote their application in real-time.

III. System Architecture and Inspection Strategy

A. Equipment

To implement ICARUS, an off-the-shelf UAV is used (DJI Matrice 300 RTK) as shown in Fig. 1, which is equipped with the multi-sensor (RGB and thermal) DJI Zenmuse H20T camera (mounted on the right downward gimbal) and the MicaSense Altum multispectral camera with the Downwelling Light Sensor (DLS) 2 (mounted on the left downward gimbal) [33]–[35]. Moreover, the UAV is capable of simultaneously receiving multiple GNSSs (GPS, Galileo, GLONASS, BeiDou), leading to improved navigation and positioning accuracy. Finally, the NVIDIA Jetson Xavier NX embedded platform (Fig. 1-inset), is mounted on top of the

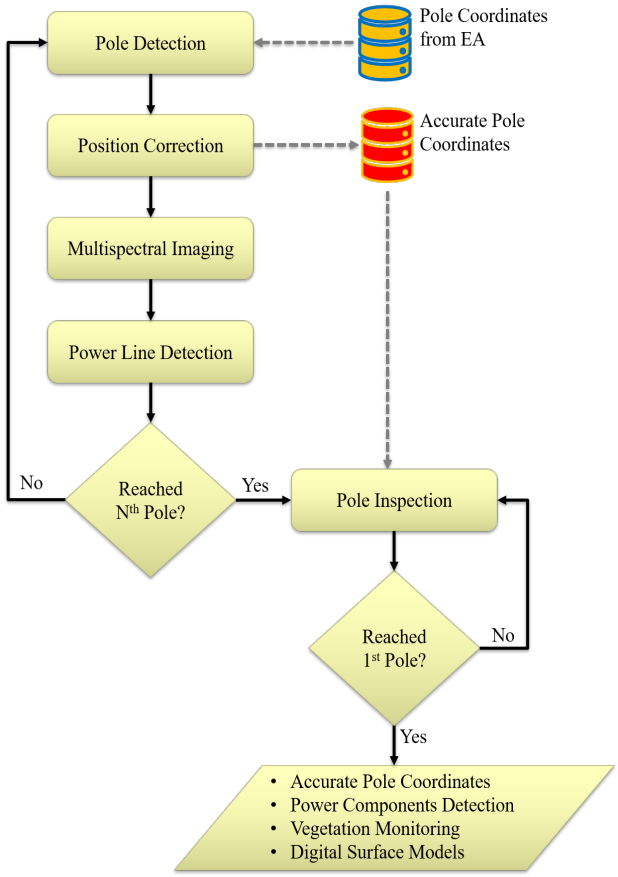

Fig. 2: Process diagram of the ICARUS platform

UAV for implementing deep learning and navigation algorithms in real-time, allowing the UAV to perform inspection procedures described in the following Section. It must be noted that the embedded platform does not affect GNSS availability, since the corresponding antennas are located on the UAV's frame arms above the propellers, as indicated by the orange dotted arrows in Fig. 1. The red dashed arrows in Fig. 1, denote the transmission antennas for communication between the UAV and the remote controller.

B. Inspection Procedure

The ICARUS toolkit implements a vision-based UAV monitoring platform for MV power distribution network inspection, as illustrated in Fig. 2. The UAV is programmed to autonomously take-off, set a course over the sequence of poles to be inspected, collect data and safely return to the take-off point. Additionally, the precise locations of the poles are not a requirement; hence, the UAV can be supplied with the best-known coordinates using e.g. maps, satellite images, and the ICARUS toolkit can correct them. In the current implementation, pole locations can be provided with a tolerance of ±9m.

1) Pole Detection

For the pole detection task, the UAV flew at a constant height of approximately 50m above ground with the camera turned downwards. To identify poles (top-view) in videos under different background and lighting conditions, the tiny-You-Only-Look-Once (tiny-YOLO) v4 was employed.

(a) (b)

Fig. 3: (a) Pole detection using the tinyYOLOv4 to process, in real-time, video frames on the NVIDIA Jetson Xavier NX embedded platform, and (b) Position correction by aligning the image center (green cross) to the center of bounding box (light blue).

YOLO is a state-of-the-art, real-time object detection system, which was initially created by Darknet, an open source deep neural network framework coded in C and CUDA [36]. The employed tiny-YOLOv4 model was selected towards real-time pole detection and was chosen over its predecessor (v3 model), since it has been shown to perform better in terms of accuracy and performance [37].

The dataset used for training consisted of top-view imagery of poles from various locations of the Electricity Authority of Cyprus MV network. Several images in the dataset were captured across different seasons to account for a variety of background and lighting conditions, such as grass or ground, cloudy or sunny weather, as well as at different heights to account for variations in the UAV's height during inspection; thus, achieving better accuracy. The detection model was trained using only one class, to detect the top-view of the pole labeled as a "pylon". For the training, we used samples containing the T-shaped bar of the pole with the insulators and the top of pole, to minimize detections of other structures on the ground, i.e. wooden logs. Table I depicts the accuracy of the tiny-YOLOv4 model trained on our dataset, using various Intersection Over Union (IOU) thresholds. To achieve the reported Mean Average Precision (MAP) and IOU percentage values, a static threshold of 0.3 for the confidence was used. As can be seen, with a value of 0.25 for the IOU threshold, the detector achieved a MAP of 92%. To minimize false positives, which might lead in inaccurate position correction, a higher confidence threshold of 0.3 was selected, after several experimentation trials. It must be emphasized that pole detection was performed in real-time, by executing tiny-YOLOv4 using the OpenCV library [38] in C++, on the Jetson Xavier NX, achieving an average performance of 20 FPS, during real inspection tasks (top left of Fig. 3). A representative example of the detection is shown in Fig. 3a, where the green cross indicates the center of the current frame, and the light blue bounding box marks the position of the pole within each frame.

TABLE I. TINY-YOLOV4 ACCURACY FOR POLE DETECTION TASK

IOU Threshold	Performance	
	MAP (%)	IOU (%)
0.25	92	92
0.5	62	84
0.75	66	32

2) Position Correction

Following pole detection, the ICARUS toolkit *online* generated suitable flight control commands, according to the control procedure shown in Fig. 4, for aligning UAV directly above the pole, i.e. the image center (green cross) coincides with the center of the bounding box (light blue) with a tolerance of 50cm, as shown in Fig. 3b. To define this tolerance, we performed a different experiment by instructing the UAV to navigate to a specific location and hover for approximately 5 minutes, where position (latitude, longitude) was recorded at a frequency of 5Hz. Analysis of the data indicated that the error (μ±σ) from the target location was 47±7.64cm; hence, we chose a value of 50cm for position correction. The control procedure (Fig. 4) consisted of identifying the position of pole using tiny-YOLOv4 in terms of its center coordinates (x_t, y_t), which were compared with

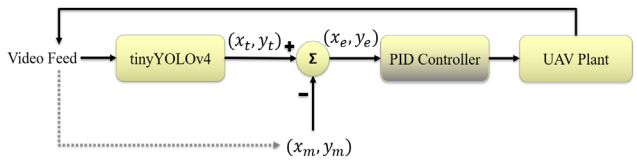

Fig. 4: High level control procedure to align UAV directly above the detected pole, i.e. center of the image (x_m, y_m) with the center of the bounding box (x_t, y_t).

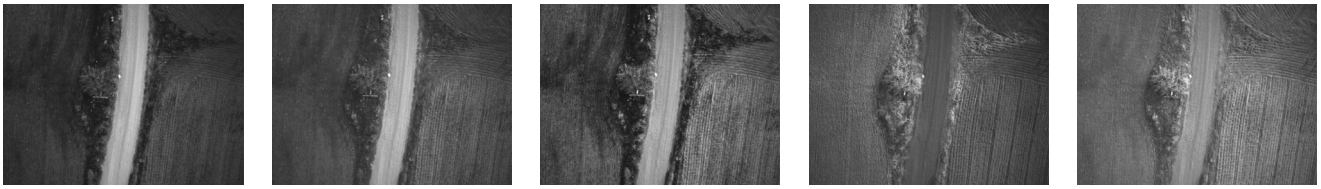

Fig. 5: Multispectral imaging of the power line corridor. From left to right the blue (475±32nm), green (560±27nm), red (668±14nm), red edge (717±12nm), and near infrared (842±57) channels are shown [35].

the coordinates of the image's center (x_m, y_m) to yield the position error (x_e, y_e), which in turn was minimized using a PID controller generating appropriate commands for the UAV to follow. At this adjusted position, spatial coordinates were recorded as the accurate coordinates of the current pole. To obtain high accuracy in recording spatial coordinates, multiple GNSSs such as GPS, Galileo, GLONASS, and BeiDou were enabled.

3) Multispectral Imaging

An important component of power infrastructure inspection, is the vegetation near and along the power line corridor, which if left unmonitored may result in electrical discharges, causing fires and damages to the network and the environment. To facilitate vegetation monitoring, a multispectral camera with five bands, i.e. blue, green, red, red edge, near infrared (NIR) was employed, and geotagged images of the power line corridor were acquired, as shown in Fig. 5. The acquired dataset was subsequently processed for estimating Normalized Difference Vegetation Index (NDVI) and Soil Adjusted Vegetation Index (SAVI) to assess vegetation condition near the power lines [39], [40]. Moreover, these images were used to create dense 3D models by employing photogrammetric techniques. To this end and to promote accurate 3D modelling, the multispectral camera was programmed to capture images with forward overlap ≥85% during UAV navigation and maximal side overlap.

NDVI is a classic approach for assessing the condition of vegetation in the inspected regions, while SAVI is an improved index accounting for different soil background conditions. Both indices are shown in (1), where L is an adjustment factor and was set to 0.5 [40]. Examples of both indices are illustrated in Fig. 6 using corresponding images shown in Fig. 5.

$$\begin{aligned} \text{NDVI} &= (\text{NIR} - \text{Red}) / (\text{NIR} + \text{Red}) \\ \text{SAVI} &= (1 + \text{L}) * (\text{NIR} - \text{Red}) / (\text{NIR} + \text{Red} + \text{L}) \end{aligned} \quad (1)$$

Additionally, the dense 3D model of the inspected power line corridor was obtained by implementing different photogrammetric techniques on the acquired dataset, using the Agisoft Metashape software [41]. A snapshot of the 3D model is presented in Fig. 7 and can be used for identifying potential obstacles within the power line corridor. Both vegetation indices and 3D model were estimated offline, after inspection mission.

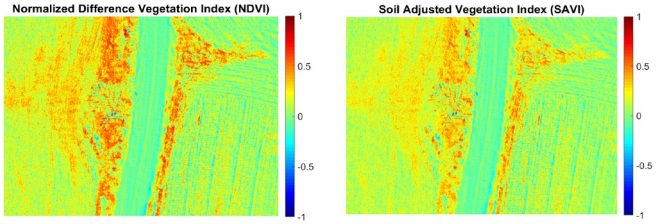

Fig. 6: NDVI (left) and SAVI (right) using images shown in Fig. 5.

4) Power Line Detection

Power line detection has been previously employed as a method for navigation; however, due to inaccuracies as a result of different background conditions, it was rendered not suitable for fully autonomous navigation [4]. In this study, we used power line detection for counting the number of lines between each pair of poles, estimating an obstacle indication factor (Obstacle Index; OI). This index complements the analysis of 3D model for detecting obstacles, and was estimated for each pair of poles by counting whether all three lines in between were detected or not. Low OI values indicated that all three lines were continuously detected in the video feed, suggesting that vegetation does not obstruct the power line corridor. Conversely, high OI values create an alarm that lines could not be detected and then the operator can manually inspect the corresponding part of the video to make the final decisions.

To identify power lines, we used the prior knowledge that these would be approximately vertical in the video feed, and developed an algorithm based on basic image filtering and morphological operations. The vertical direction of power lines was achieved by turning the UAV to the next pole's yaw before navigating from the current to the next pole. Since, the UAV was flying 50m above ground, RGB video from the DJI Zenmuse H20T was acquired, which has optical zoom capabilities, in an attempt to better distinguish power lines from the background.

ALGORITHM 1: ALGORITHM TO IDENTIFY POWER LINES IN RGB VIDEO

1: **procedure** LINE DETECTION (frame)
2: Convert frame from RGB to grayscale
3: Detect edges with Laplacian kernel L_k
4: Apply hit-miss transform to discard noisy lines using structuring elements B_1 and B_2
5: Apply morphological opening to filter detected lines with structuring element B_3
6: Identify lines using probabilistic Hough transform [42]
7: Discard lines which have length shorter than 50 pixels, and keep lines whose angle of orientation is between 85° and 95°

with $L_k = \begin{pmatrix} 0 & 1 & 0 \\ 1 & -4 & 1 \\ 0 & 1 & 0 \end{pmatrix}, B_1 = \begin{pmatrix} 0 & 1 & 0 \\ 0 & 1 & 0 \\ 0 & 1 & 0 \\ 0 & 1 & 0 \\ 0 & 1 & 0 \\ 0 & 1 & 0 \\ 0 & 1 & 0 \end{pmatrix}, B_2 = \begin{pmatrix} 1 & 0 & 1 \\ 1 & 0 & 1 \\ 1 & 0 & 1 \\ 1 & 0 & 1 \\ 1 & 0 & 1 \\ 1 & 0 & 1 \\ 1 & 0 & 1 \end{pmatrix}, B_3 = \begin{pmatrix} 1 \\ 1 \\ 1 \\ 1 \\ 1 \end{pmatrix}$

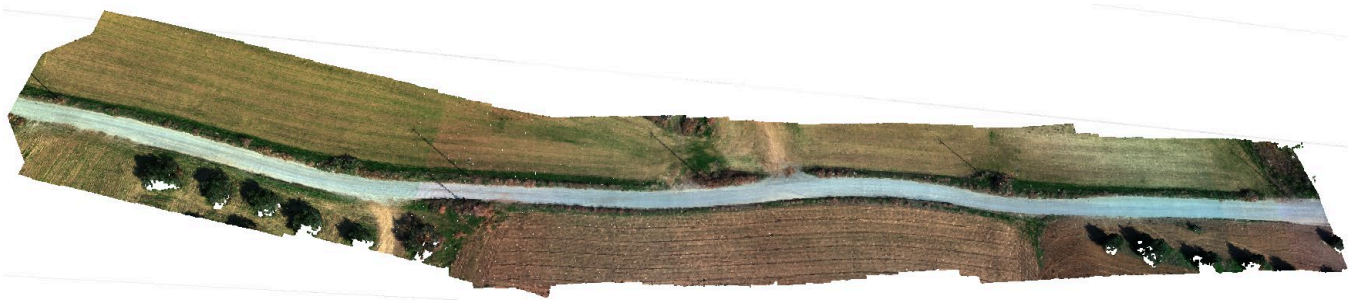

Fig. 7: Dense 3D model resulted by implementing photogrammetric algorithms on the multispectral dataset.

The algorithm was applied to each one frame as described in Algorithm 1. Specifically, following conversion of RGB image to grayscale, edges were detected using the Laplacian operator, without applying filtering, e.g. Gaussian smoothing, to avoid blurring the power lines. We opted for Laplacian instead of alternative first-order-difference operators, e.g. Sobel, Prewitt, to detect the edges using a single kernel instead of two as in the latter case, for minimizing processing time, despite the fact that currently these algorithms are applied offline. The incentive for such approach was to ultimately perform real-time power line detection on the NVIDIA Jetson Xavier NX platform.

The result of edge detection consisted of noisy edges as well; hence, we applied the hit-miss transform to discard any spurious lines, according to (2).

$$A \odot B = (A \ominus B_1) \cap (A^c \ominus B_2) \quad (2)$$

where $\ominus$ is the erosion operator, A^c denotes the complement and $B = (B_1, B_2)$, where B_1 and B_2 operate on the foreground and background, respectively, and are defined in Algorithm 1. The motivation for defining such a kernel, is that we aimed at identifying those pixels in the foreground which are vertically connected (*hit* with structuring element B_1) and at the same time their adjacent pixels belong to the background (*miss* with structuring element B_2). Following the hit-miss transform, a morphological opening operation with a vertical structuring element was additionally applied, to refine the detected power lines as described in (3).

$$A \circ B_3 = (A \ominus B_3) \oplus B_3 \quad (3)$$

where $\oplus$ is the dilation operation and B_3 is defined in Algorithm 1. The procedure is illustrated in Fig. 8, including the initial RGB (Fig. 8a) and the corresponding grayscale image (Fig. 8b). The application of Laplacian operator yielded in a very noisy result (Fig. 8c) due to the absence of smoothing; nevertheless, the structure of interest (power lines) can be still visually identified (they are vertically oriented in the image). The extraction of power lines was achieved by applying the hit-miss transform (Fig. 8d) using properly designed structuring elements B_1 and B_2, while the application of morphological opening (Fig. 8e) aimed at refining the obtained results for providing probabilistic Hough transform with best estimates of the lines. Finally, the identified power lines are shown in green in Fig. 8f after applying two filtering criteria with respect to the length and orientation of lines, as mentioned in Algorithm 1 (step 7). Additional power line detection results are shown in Fig. A1 of the Appendix.

Apart from the aforementioned algorithm to detect power lines, we also examined alternative algorithms commonly employed for power line detection, such as the use of Canny edge detector instead of Laplacian (step 3 in Algorithm 1), the LSD and Edge Drawing (ED) algorithms [31], [43]. In this case, comparisons were made in terms of OI, since in the inspected region no obstacles were within the power line corridor, as well as in terms of processing time.

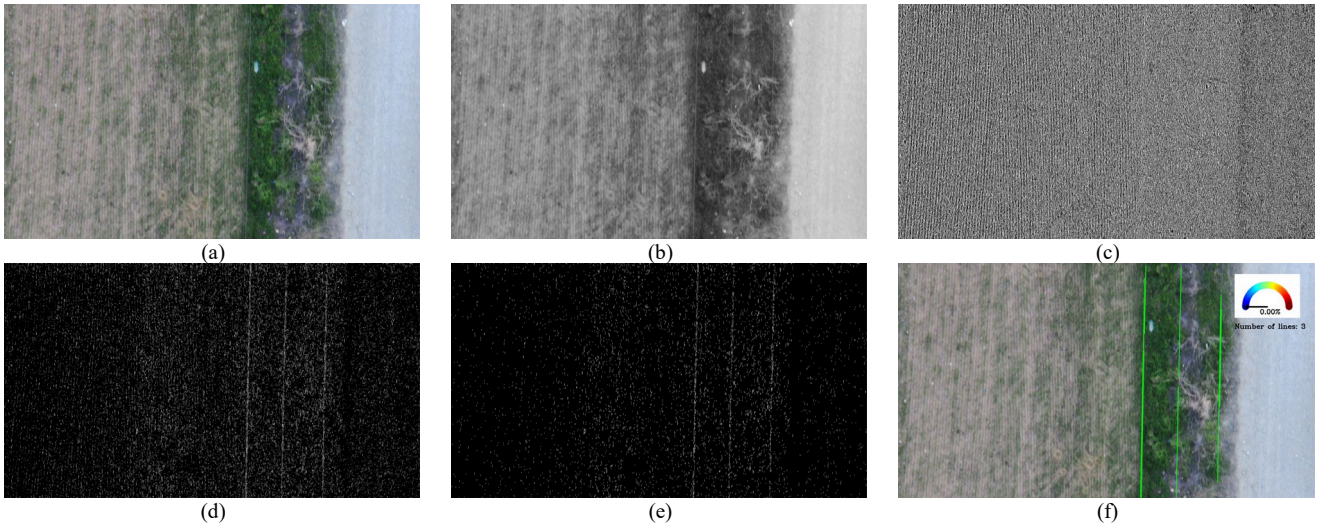

Fig. 8: Procedure for detecting power lines including the (a) initial RGB image, (b) corresponding grayscale image, (c) application of Laplacian operator to detect edges, (d) application of hit-miss transform to identify power lines, (e) application of morphological opening to refine results of hit-miss transform and (f) the finally detected lines, shown in green, using the probabilistic Hough transform.

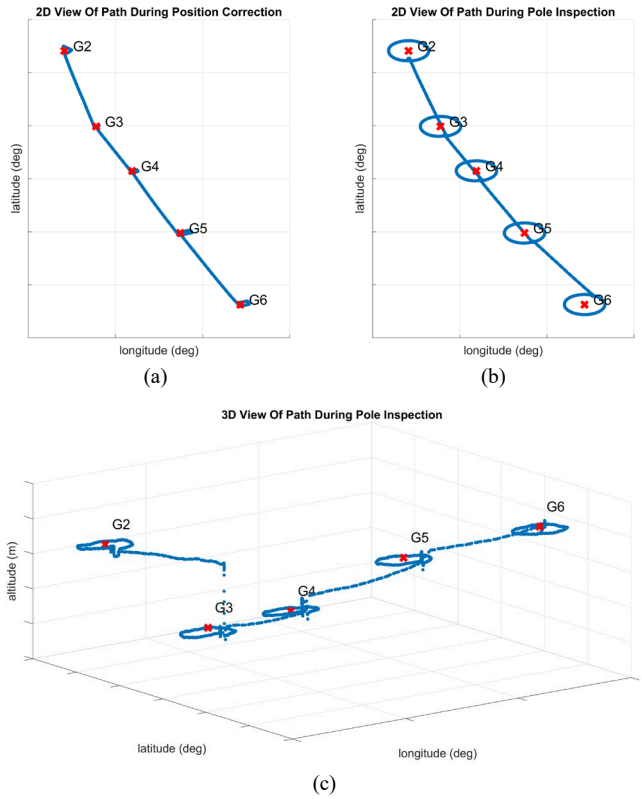

Fig. 9: 2D trajectories during (a) position correction and (b) pole inspection, and (c) 3D trajectory for inspecting each pole separately. Red marks indicate the position of poles, also identified by their IDs, while in (a) movements near the poles demonstrate position correction. The locations of the poles are not disclosed due to confidentiality reasons.

The corresponding results are illustrated in Table II, where inspected poles are identified by their unique IDs, i.e. G2, G3, G4, G5 and G6. Algorithms were executed offline, on the same reference computer with an Intel i5-7300 CPU, 8GB RAM running Ubuntu Linux operating system. As can be seen for the inspected poles, the Laplacian approach yielded similar, and marginally better results in some cases, for the OI, to the other methods at a significantly lower processing time.

TABLE II. PERFORMANCE OF ALGORITHMS IN IDENTIFYING POWER LINES, IN TERMS OF OBSTACLE INDEX (OI) AND EXECUTION TIME

Method	Pole Pair	OI (%)	Average Execution Time (ms/frame)
Laplacian	G2-G3	10.70	58
	G3-G4	15.15	52
	G4-G5	10.49	52
	G5-G6	12.01	60
Canny	G2-G3	10.36	184
	G3-G4	15.76	153
	G4-G5	8.71	157
	G5-G6	12.01	187
LSD [31]	G2-G3	11.31	143
	G3-G4	21.26	178
	G4-G5	6.57	172
	G5-G6	10.78	199
ED [43]	G2-G3	17.45	183
	G3-G4	82.42	188
	G4-G5	0	174
	G5-G6	30.12	204

Fig. 10: Power components detection (insulators, pole; top-panel) and thermal imaging (bottom-panel)

5) Pole Inspection

Following identification and adjustment of the spatial coordinates of a set of poles, the UAV initiated a "*Return Back*" command using the corrected coordinates, to navigate to each pole for performing a more fine-grained inspection, acquiring high-quality data from the vision sensors. In this case, the navigation path differed from the path followed during the previous tasks, by following a cyclical trajectory above each pole, to acquire video footages from RGB and thermal sensors to provide a 360° view, for identifying power components and conditions of increased temperature. An example of the 2D trajectory is shown in Fig. 9a-b for position correction and pole inspection, respectively, while Fig. 9c illustrates the 3D trajectory during pole inspection, where the UAV navigated above each pole in a circular motion, also considering changes in terrain height. The locations of the poles are not disclosed due to confidentiality reasons.

The acquired thermal and RGB video footages were both processed offline. Analyzing thermal videos, assists in identifying faulty power components, by recognizing increased temperature of the T-shaped bar on each pole. In Fig. 10-bottom panel, a representative example of image from the thermal camera is illustrated. On the other hand, RGB videos were processed to identify the power components, e.g. insulators and the pole itself, for detecting defects.

To this end, a new detection model was trained based on the full YOLOv4 model instead of the tiny-YOLOv4, to achieve superior accuracy. Training dataset consisted of 1000 images, which were exported from the corresponding RGB videos, from various poles during testing of the implementation. The model was trained to detect the pole and different kinds of insulators, as shown in Fig. 10-top panel, using IOU and confidence thresholds of 0.5, achieving a MAP of 79.2%. Post-processing of detection results can provide further information on the condition of insulators by identifying defects, such as cracks.

6) System Output

The output of the inspection procedure was analyzed to provide actionable decisions related to proactive maintenance of the power network, and consisted of a status report with the accurate spatial coordinates of the poles, the detection of power components (Fig. 10-upper panel), such as different types of insulators and the pole itself, which along with thermal imaging data (Fig. 10-lower panel) were employed to identify degraded material. Moreover, the multispectral dataset was processed to calculate vegetation indices (Fig. 6) and generate 3D models of the power line corridor (Fig. 7), which along with power line detection were used for identifying potential obstacles near the power lines. In the status report all visited poles are documented and identified by their unique ID (as provided by EAs) and their accurate coordinates with 10 digits precision. Additional information includes whether the pole could be detected during the "*Pole Detection*" task, as well as the estimated OI values, corresponding to the detection of power lines.

IV. Conclusions And Future Work

In this study we presented ICARUS; an automatic autonomous power infrastructure inspection approach using UAV. ICARUS integrates multiple vision sensors, is equipped with a state-of-the-art embedded platform to facilitate real-time data processing, and is based on a hybrid navigation approach (multiple GNSSs and vision-based) to perform inspection. With this approach, acquisition of high-quality data was facilitated in a safe and fast manner, and was applied for autonomously inspecting part of the MV distribution network in Cyprus with a promising outlook. A video demonstration of ICARUS can be found at https://youtu.be/MgzHVPYRyfU.

As a future work, we aim to implement algorithms for processing visible-light data in order to detect both faulty insulators and poles, as well as to detect increased temperatures using the thermal video feeds. Importantly, in the latter case, a change in the trajectory of the UAV is deemed necessary for acquiring thermal data such that power components are better visible, since resolution of thermal camera is quite low. Moreover, algorithms will be implemented for processing the 3D surface models to identify and record the exact location of obstacles that likely exist within the power line corridor.

Appendix

Fig. A1 presents additional examples of power line detection (indicated in green) of the proposed method based on the Laplacian operator.

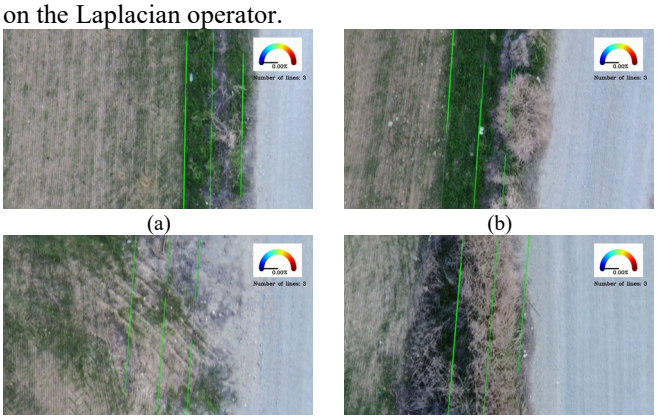

Fig. A1: Additional examples of the power line detection algorithm based on the Laplacian operator. The successful detection of lines is indicated by the green color, while in each case the total number of lines is counted.

Acknowledgments

This work has been supported by the European Union's Horizon 2020 research and innovation programme under grant agreement No 739551 (KIOS CoE) and from the Government of the Republic of Cyprus through the Directorate General for European Programmes, Coordination and Development. We would like to thank Electricity Authority of Cyprus for providing the locations to acquire data used in the present study, Athina Silvestrou for conducting photogrammetric analysis and Petros Petrides for assisting in data acquisition.

References

[1] L. Matikainen *et al.*, "Remote sensing methods for power line corridor surveys," *ISPRS Journal of Photogrammetry and Remote Sensing*, vol. 119. Elsevier B.V., pp. 10–31, Sep. 01, 2016, doi: 10.1016/j.isprsjprs.2016.04.011.

[2] Ari Kahan, "Global electricity consumption continues to rise faster than population." https://www.eia.gov/todayinenergy/detail.php?id=44095 (accessed Jan. 19, 2021).

[3] A. B. Alhassan, X. Zhang, H. Shen, and H. Xu, "Power transmission line inspection robots: A review, trends and challenges for future research," *International Journal of Electrical Power and Energy Systems*, vol. 118. Elsevier Ltd, p. 105862, Jun. 01, 2020, doi: 10.1016/j.ijepes.2020.105862.

[4] V. N. Nguyen, R. Jenssen, and D. Roverso, "Automatic autonomous vision-based power line inspection: A review of current status and the potential role of deep learning," *Int. J. Electr. Power Energy Syst.*, vol. 99, pp. 107–120, Jul. 2018, doi: 10.1016/j.ijepes.2017.12.016.

[5] M. Bruch, V. Münch, M. Aichinger, M. Kuhn, M. Weymann, and G. Schmid, "Power Blackout Risks." [Online]. Available: https://www.thecroforum.org/wp-content/uploads/2012/09/CRO-Position-Paper-Power-Blackout-Risks-1-1.pdf.

[6] J. Katrasnik, F. Pernus, and B. Likar, "A Survey of Mobile Robots for Distribution Power Line Inspection," *IEEE Trans. Power Deliv.*, vol. 25, no. 1, pp. 485–493, Jan. 2010, doi: 10.1109/TPWRD.2009.2035427.

[7] J. Del-Cerro, I. Aguirre, and A. Barrientos, "Development of a low-cost autonomous minihelicoptor for power line inspections," in *Mobile Robots XV and Telemanipulator and Telepresence Technologies VII*, Mar. 2001, vol. 4195, pp. 1–7, doi: 10.1117/12.417291.

[8] I. Golightly and D. Jones, "Visual control of an unmanned aerial vehicle for power line inspection," in *2005 International Conference on Advanced Robotics, ICAR '05, Proceedings*, 2005, vol. 2005, pp. 288–295, doi: 10.1109/ICAR.2005.1507426.

[9] X. Hui, J. Bian, Y. Yu, X. Zhao, and M. Tan, "A novel autonomous navigation approach for UAV power line inspection," in *2017 IEEE International Conference on Robotics and Biomimetics, ROBIO 2017*, Mar. 2018, vol. 2018-January, pp. 1–6, doi: 10.1109/ROBIO.2017.8324488.

[10] J. Bian, X. Hui, X. Zhao, and M. Tan, "A Novel Monocular-Based Navigation Approach for UAV Autonomous Transmission-Line Inspection," in *IEEE International Conference on Intelligent Robots and Systems*, Dec. 2018, pp. 6207–6213, doi: 10.1109/IROS.2018.8593926.

[11] X. Zhao, M. Tan, X. Hui, and J. Bian, "Deep-learning-based autonomous navigation approach for UAV transmission line inspection," in *Proceedings - 2018 10th International Conference on Advanced Computational Intelligence, ICACI 2018*, Jun. 2018, pp. 455–460, doi: 10.1109/ICACI.2018.8377502.

[12] X. Hui, J. Bian, X. Zhao, and M. Tan, "Vision-based autonomous navigation approach for unmanned aerial vehicle transmission-line inspection," *Int. J. Adv. Robot. Syst.*, vol. 15, no. 1, p. 172988141775282, Jan. 2018, doi: 10.1177/1729881417752821.

[13] D. Jones, I. Golightly, J. Roberts, and K. Usher, "Modeling and control of a robotic power line inspection vehicle," in *Proceedings of the IEEE International Conference on Control Applications*, 2006, pp. 632–637, doi: 10.1109/CACSD-CCA-ISIC.2006.4776719.

[14] B. Wang, L. Han, H. Zhang, Q. Wang, and B. Li, "A flying robotic system for power line corridor inspection," in *2009 IEEE International Conference on Robotics and Biomimetics, ROBIO 2009*, 2009, pp. 2468–2473, doi: 10.1109/ROBIO.2009.5420421.

[15] B. Wang, X. Chen, Q. Wang, L. Liu, H. Zhang, and B. Li, "Power line inspection with a flying robot," in *2010 1st International Conference on Applied Robotics for the Power Industry, CARPI 2010*, 2010, doi: 10.1109/CARPI.2010.5624430.

[16] S. Hrabar, T. Merz, and D. Frousheger, "Development of an autonomous helicopter for aerial powerline inspections," in *2010 1st International Conference on Applied Robotics for the Power Industry, CARPI 2010*, 2010, doi: 10.1109/CARPI.2010.5624432.

[17] C. Deng, J. Y. Liu, Y. B. Liu, and Y. Y. Tan, "Real time autonomous transmission line following system for quadrotor helicopters," in *2016 International Conference on Smart Grid and Clean Energy Technologies, ICSGCE 2016*, Mar. 2017, pp. 61–64, doi: 10.1109/ICSGCE.2016.7876026.

[18] Z. Li, Y. Liu, R. Walker, R. Hayward, and J. Zhang, "Towards automatic power line detection for a UAV surveillance system using pulse coupled neural filter and an improved Hough transform," *Mach. Vis. Appl.*, vol. 21, no. 5, pp. 677–686, Aug. 2010, doi: 10.1007/s00138-009-0206-y.

[19] Y. Liu, L. Mejias, and Z. Li, "Fast Power Line Detection And Localization Using Steerable Filter For Active UAV Guidance," *ISPRS - Int. Arch. Photogramm. Remote Sens. Spat. Inf. Sci.*, vol. XXXIX-B3, pp. 491–496, Aug. 2012, doi: 10.5194/isprsarchives-xxxix-b3-491-2012.

[20] A. Ceron, I. F. Mondragon B., and F. Prieto, "Power line detection using a circle based search with UAV images," in *2014 International Conference on Unmanned Aircraft Systems, ICUAS 2014 - Conference Proceedings*, 2014, pp. 632–639, doi: 10.1109/ICUAS.2014.6842307.

[21] A. Cerón, I. Mondragón, and F. Prieto, "Onboard visual-based navigation system for power line following with UAV," *Int. J. Adv. Robot. Syst.*, vol. 15, no. 2, p. 172988141876345, Mar. 2018, doi: 10.1177/1729881418763452.

[22] A. Zormpas *et al.*, "Power transmission lines inspection using properly equipped Unmanned Aerial Vehicle (UAV)," in *IST 2018 - IEEE International Conference on Imaging Systems and Techniques, Proceedings*, Dec. 2018, doi: 10.1109/IST.2018.8577142.

[23] G. Zhou, J. Yuan, I. L. Yen, and F. Bastani, "Robust real-time UAV based power line detection and tracking," in *Proceedings - International Conference on Image Processing, ICIP*, Aug. 2016, vol. 2016-August, pp. 744–748, doi: 10.1109/ICIP.2016.7532456.

[24] X. Zhang, G. Xiao, K. Gong, J. Zhao, and D. P. Bavirisetti, "Automatic Power Line Detection for Low-Altitude Aircraft Safety Based on Deep Learning," in *Proceedings of International Conference on Aerospace System Science and Engineering 2018*, 2019, pp. 169–183.

[25] V. N. Nguyen, R. Jenssen, and D. Roverso, "LS-Net: fast single-shot line-segment detector," *Mach. Vis. Appl.*, vol. 32, no. 1, pp. 1–16, Feb. 2021, doi: 10.1007/s00138-020-01138-6.

[26] H. Choi, G. Koo, B. J. Kim, and S. Woo Kim, "Real-time Power Line Detection Network using Visible Light and Infrared Images," in *International Conference Image and Vision Computing New Zealand*, Dec. 2019, vol. 2019-December, doi: 10.1109/IVCNZ48456.2019.8961002.

[27] I. Golightly and D. Jones, "Corner detection and matching for visual tracking during power line inspection," *Image Vis. Comput.*, vol. 21, no. 9, pp. 827–840, Sep. 2003, doi: 10.1016/S0262-8856(03)00097-0.

[28] C. Martinez, C. Sampedro, A. Chauhan, and P. Campoy, "Towards autonomous detection and tracking of electric towers for aerial power line inspection," in *2014 International Conference on Unmanned Aircraft Systems, ICUAS 2014 - Conference Proceedings*, 2014, pp. 284–295, doi: 10.1109/ICUAS.2014.6842267.

[29] C. Sampedro, C. Martinez, A. Chauhan, and P. Campoy, "A supervised approach to electric tower detection and classification for power line inspection," in *Proceedings of the International Joint Conference on Neural Networks*, Sep. 2014, pp. 1970–1977, doi: 10.1109/IJCNN.2014.6889836.

[30] O. Araar, N. Aouf, and J. L. V. Dietz, "Power pylon detection and monocular depth estimation from inspection UAVs," *Ind. Rob.*, vol. 42, no. 3, pp. 200–213, May 2015, doi: 10.1108/IR-11-2014-0419.

[31] R. Grompone Von Gioi, J. Jakubowicz, J. M. Morel, and G. Randall, "LSD: A fast line segment detector with a false detection control," *IEEE Trans. Pattern Anal. Mach. Intell.*, vol. 32, no. 4, pp. 722–732, Apr. 2010, doi: 10.1109/TPAMI.2008.300.

[32] J. I. Larrauri, G. Sorrosal, and M. Gonzalez, "Automatic system for overhead power line inspection using an Unmanned Aerial Vehicle - RELIFO project," in *2013 International Conference on Unmanned Aircraft Systems, ICUAS 2013 - Conference Proceedings*, 2013, pp. 244–252, doi: 10.1109/ICUAS.2013.6564696.

[33] DJI, "Matrice 300 RTK – Built Tough. Works Smart. – DJI," 2020. https://www.dji.com/matrice-300 (accessed Jan. 21, 2021).

[34] DJI, "Zenmuse H20 Series – Unleash the Power of One – DJI," 2020. https://www.dji.com/zenmuse-h20-series (accessed Jan. 21, 2021).

[35] MicaSense, "Altum - MicaSense," 2020. https://micasense.com/altum/ (accessed Jan. 21, 2021).

[36] J. Redmon, S. Divvala, R. Girshick, and A. Farhadi, "You only look once: Unified, real-time object detection," in *Proceedings of the IEEE Computer Society Conference on Computer Vision and Pattern Recognition*, Dec. 2016, vol. 2016-December, pp. 779–788, doi: 10.1109/CVPR.2016.91.

[37] A. Bochkovskiy, C.-Y. Wang, and H.-Y. M. Liao, "YOLOv4: Optimal Speed and Accuracy of Object Detection," *arXiv*, Apr. 2020, Accessed: Feb. 03, 2021. [Online]. Available: http://arxiv.org/abs/2004.10934.

[38] A. Kaehler and G. Bradski, *Learning OpenCV - Computer Vision in C++ with the OpenCV Library*, 1st ed., vol. 53, no. 9. O'Reilly Media, Inc., 2016.

[39] J. W. . J. Rouse, R. H. Haas, J. A. Schell, and D. W. Deering, "Monitoring Vegetation Systems in the Great Plains with Erts," *Proceedings, 3rd Earth Resour. Technol. Satell. Symp.*, vol. 351, p. 317, 1974.

[40] A. R. Huete, "A soil-adjusted vegetation index (SAVI)," *Remote Sens. Environ.*, vol. 25, no. 3, pp. 295–309, Aug. 1988, doi: 10.1016/0034-4257(88)90106-X.

[41] Agisoft, "Agisoft Metashape," no. September, p. 160, 2020, Accessed: Jan. 27, 2021. [Online]. Available: https://www.agisoft.com/.

[42] J. Matas, C. Galambos, and J. Kittler, "Robust detection of lines using the progressive probabilistic hough transform," *Comput. Vis. Image Underst.*, vol. 78, no. 1, pp. 119–137, Apr. 2000, doi: 10.1006/cviu.1999.0831.

[43] C. Topal, C. Akinlar, and Y. Genç, "Edge drawing: A heuristic approach to robust real-time edge detection," in *Proceedings - International Conference on Pattern Recognition*, 2010, pp. 2424–2427, doi: 10.1109/ICPR.2010.593.